Boltzmann-equation approach to the negative magnetoresistance of ferromagnetic–normal-metal multilayers

Randolph Q. Hood and L. M. Falicov
Department of Physics, University of California, Berkeley, California 94720
and Materials Sciences Division, Lawrence Berkeley Laboratory, Berkeley, California 94720
(Received 7 April 1992)

The Boltzmann equation is solved for a system consisting of a ferromagnetic–normal-metal–ferromagnetic metallic trilayer. The in-plane conductance of the film is calculated for two configurations: the ferromagnetic layers aligned (i) parallel and (ii) antiparallel to each other. The results explain the giant negative magnetoresistance encountered in these systems when an initial antiparallel arrangement is changed into a parallel configuration by application of an external magnetic field. The calculation depends on (a) geometric parameters (the thicknesses of the layers), (b) intrinsic metal parameters (number of conduction electrons, magnetization, and effective masses in the layers), (c) bulk sample properties (conductivity relaxation times), (d) interface scattering properties (diffuse scattering versus potential scattering at the interfaces), and (e) outer surface scattering properties (specular versus diffuse surface scattering). For perfect specular scattering at the surfaces the problem becomes identical to an infinite multilayer, periodic system. It is found that a large negative magnetoresistance requires, in general, considerable asymmetry in the interface scattering for the two spin orientations. All qualitative features of the experiments are reproduced. Quantitative agreement can be achieved with sensible values of the parameters. The effect can be conceptually explained based on considerations of phase-space availability for an electron of a given spin orientation as it travels through the multilayer sample in the various configurations.

I. INTRODUCTION

Ferromagnetic–normal-metal superlattices and sandwiches[1,2] display a number of interesting properties, such as a varying interlayer magnetic coupling[3] and a giant negative magnetoresistance (MR) effect.[4] It has been found that in systems such as $(Fe/Cr)_n$, the magnetic moments of each Fe layer are arranged with respect to the neighboring layers either in a parallel fashion, or in an antiparallel one, depending on the thickness of the Cr spacers and on the quality of the Fe/Cr interfaces.[3,5,6]

When the conditions are such that the consecutive moments are arranged antiparallel to each other, the application of an external magnetic field to the sample results in two effects: (1) the moments rearrange themselves into a completely parallel arrangement in fields of the order of 1 T; and (2) the sample decreases its resistance—negative MR—in all directions (in-plane in particular) by varying amounts which can be as small as a few percent, and as large as 50% (for Fe/Cr at liquid-helium temperatures). This latter is known as the giant magnetoresistance effect (GMR).

Even though the current knowledge of the MR effect is incomplete, one fact that has emerged is that spin-dependent interfacial scattering plays an important role. Experiments by Fullerton *et al.*[7] indicate that increased interfacial roughness enhances the GMR. Baumgart *et al.*[8] have found that ultrathin layers of elements (V, Mn, Ge, Ir, and Al) deposited at the Fe-Cr interface lead to changes in the MR, which correlate with the ratio of spin-up and spin-down resistivities arising from spin-dependent impurity scattering of these elements when alloyed with Fe. This result is in agreement with the suggestion of Baibich *et al.*[4] that the spin dependence of impurity scattering at the interfaces is related to that observed[9] in alloyed ferromagnetic metals such as Ni, Fe, and Co.

By fitting MR data of epitaxially grown Fe(001)/Cr(001) multilayers to model-calculation results, Levy, Zhang, and Fert[10] concluded that the ratio of the interfacial resistivity to bulk resistivity is 0.83. Further confirmation of the importance of the interface in the MR effect was provided by Barthélémy *et al.*,[11] who point out that the experimental data they obtained for epitaxially grown Fe(001)/Cr(001) multilayers seem to be in agreement with the variation of the MR with

$$\exp(-t_{CR}/\lambda^*) ,$$

where t_{Cr} is the thickness of Cr layer and λ^* is a length of the order of the mean free path. Such a variation of the MR with layer thickness is expected from spin-dependent interface scattering. In contrast with this, if spin-dependent scattering occurred within the Fe layers, a variation of the form

$$\exp[-(t_{Fe}+2t_{Cr})/\lambda^*]$$

would be expected. Barnaś *et al.*[12] compared experimental data with their theoretical model, based on the Boltzmann transport equation with spin-dependent bulk and interface scattering, and concluded that the experimental data favor the interface contribution as being the

dominant one.

Camley and Barnaś's model[12,13] description of the MR effect, despite being one of the more complete thus far proposed, makes a number of unsuitable approximations, in particular with respect to interfacial scattering. They (a) neglect the difference in phase space available for scattering of electrons with different spin; and (b) they neglect the angular dependence of the transmission and reflection coefficients at the interfaces.

It should be emphasized that it is important to distinguish between the concepts of spin-flip scattering and spin-dependent scattering. The first refers to an event in which, during scattering, an electron reverses its spin orientation; such a phenomenon is normally caused by spin-orbit effects and/or by scattering from impurities with a localized magnetic moment. Spin-flip scattering is neglected in this contribution. The second one refers to the fact that electrons with different spin orientations experience different potentials and have different phase-space distributions. Consequently they have very different scattering cross sections both in the bulk and at the interfaces. This is extremely relevant for the purposes of this study.

Given the importance of such scattering, it is the aim of this contribution to present a model that incorporates spin-dependent interfacial scattering in a more realistic way. While the model presented here is similar in many respects to that of Camley and Barnaś, it does not suffer from the same shortcomings in its description of interfacial scattering. Utilization of a more accurate description of the interface permits a study and separation of the various scattering mechanisms and their relevance in the MR effect.

The present model, an extension of the Fuchs-Sondheimer theory,[14,15] uses a Stoner description[16] of the itinerant ferromagnetic Fe layers: It introduces different potentials for majority and minority spins. Band-structure and electron-density effects are included only by means of a constant, metal- and spin-dependent potential, and an isotropic effective mass for each spin in each layer. The different potentials in neighboring layers results in coherent potential scattering (i.e., refraction) of electrons as they traverse the interface. It has been suggested[8] that this effect alone could account for the observed spin-dependent transport properties and the oscillatory effects with layer thickness.[5] Spin-dependent potentials are also responsible for different densities of states at the Fermi level, i.e., different available phase space for the two different spin orientations. This spin-dependent scattering mechanism was found to be important to describe correctly the MR caused by domain-wall scattering in ferromagnetic materials.[17] The angular-dependent effects are treated by a quantum-mechanical matching of the electron wave functions at the interfaces. Impurity scattering at the interface and interfacial roughness are also a source of spin-dependent scattering, and they contribute to the present model through a single spin-dependent parameter, in a way similar to that used by Camley and Barnaś.

The model here also permits a comparison between Fe-Cu and Fe-Cr sandwiches and explains why, although the two systems have many similarities (e.g., long-range oscillatory interlayer coupling), they exhibit a large difference in MR properties.

The model predicts the dependence of the MR on the thickness of the layers, on the quality of the samples (mean free path) and on the quality (roughness) of the surfaces and interfaces.

In Sec. II a detailed description of the model is given. In Sec. III results are presented. Section IV contains the discussion and conclusions.

II. THE MODEL

The in-plane conductivity has been calculated for three-layer sandwich structures. Figure 1 shows the system and defines the axes and geometric parameters. Both the current and the time-independent electric field are in the $\hat{x}$ direction. A sandwich consists of three flat layers (labeled 1, 2, and 3) of infinite extent in the $\hat{x}$ and the $\hat{y}$ directions of thicknesses d_1, d_2, and d_3. The structures investigated have identical ferromagnetic materials in layers 1 and 3 and a normal metal in layer 2. The symbols α and β are used to denote the surfaces of layers 1 and 3 with the vacuum, respectively, and A and B denote the 1-2 and 2-3 interfaces, respectively.

For a given sandwich the conductivity was calculated for both antiparallel alignment, denoted $\sigma_{\uparrow\downarrow}$, and for parallel alignment, denoted $\sigma_{\uparrow\uparrow}$, of the ferromagnetic moments of layers 1 and 3. Antiparallel alignment of ferromagnetic layers in the absence of applied magnetic fields has been observed in Fe-Cr and Fe-Cu multilayers[5,18] and is believed to be caused by an antiferromagnetic interlayer coupling.[3,18] Application of a sufficiently large magnetic field causes the magnetic moments to align parallel to one another. The magnetoresistance $(\Delta\rho/\rho)$, is defined by

$$\frac{\Delta\rho}{\rho} \equiv \frac{\rho_{\uparrow\downarrow}-\rho_{\uparrow\uparrow}}{\rho_{\uparrow\downarrow}} = \frac{\sigma_{\uparrow\uparrow}-\sigma_{\uparrow\downarrow}}{\sigma_{\uparrow\uparrow}} , \tag{1}$$

where $\rho_{\mu,\nu}=(\sigma_{\mu,\nu})^{-1}$. Note that this quantity varies between zero and one (or 0 and 100 %) whenever the resis-

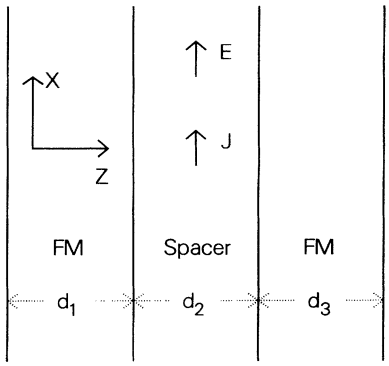

FIG. 1. Schematic diagram of the ferromagnetic–normal-metal–ferromagnetic metallic trilayer. Axes and thicknesses are defined.

tance decreases upon the application of an external magnetic field.[19]

The conductivity for both alignments is obtained by adding the contributions of the spin-up and the spin-down electrons, calculated separately. This is the two-current model,[9] which provides a good description of electron transport in magnetic $3d$ metals. As mentioned in the introduction, spin-flip processes, which mix the two currents, are neglected. It is known that their effect is small at low temperatures.[9]

The electrons involved in transport are regarded as free-electron-like with spherical Fermi surfaces. Within each layer the electrons move in a constant potential $V_{i\sigma}$, which depends on the particular layer i and the spin σ of the electron.

The electron distribution function within each layer i and for each spin σ is written in the form

$$f_{i\sigma}(\mathbf{v},z)=f^0_{i\sigma}(\mathbf{v})+g_{i\sigma}(\mathbf{v},z)\ , \tag{2}$$

which is independent of x and y by symmetry. In (2), the first term $f^0_{i\sigma}(\mathbf{v})$ is the equilibrium distribution in the absence of an electric field, and $g_{i\sigma}(\mathbf{v},z)$ is the deviation from that equilibrium in the presence of the electric field. For an electric field of magnitude E in the $\hat{x}$ direction, the Boltzmann equation in the relaxation-time approximation reduces to

$$\frac{\partial g_{i\sigma}}{\partial z}+\frac{g_{i\sigma}}{\tau_{i\sigma}v_z}=\frac{|e|E}{m_{i\sigma}v_z}\frac{\partial f^0_{i\sigma}}{\partial v_x}\ , \tag{3}$$

where $\tau_{i\sigma}$ is the relaxation time in layer i for spin σ, and e is the charge of the electron. The second-order term, proportional to $(E\times g_{i\sigma})$, has been discarded since nonlinear effects (deviations from Ohm's law) are neglected. The Lorentz-force term, proportional to $(\mathbf{v}\times\mathbf{H}/c)$, has also been dropped from the Boltzmann equation since it gives an effect which is orders of magnitude smaller than those considered here.[12]

Because of the boundary conditions it is useful to divide $g_{i\sigma}$ into two parts: $g^+_{i\sigma}(\mathbf{v},z)$ if $v_z\geq 0$ and $g^-_{i\sigma}(\mathbf{v},z)$ if $v_z<0$. The general solution to Eq. (3) takes the form

$$g^{\pm}_{i\sigma}(\mathbf{v},z)=\frac{|e|\tau_{i\sigma}E}{m_{i\sigma}}\frac{\partial f^0(\mathbf{v})}{\partial v_x}\{1+F^{\pm}_{i\sigma}(\mathbf{v})e^{\mp z/(\tau_{i\sigma}|v_z|)}\}\ , \tag{4}$$

where the functional form of $F_{i\sigma}(\mathbf{v})$ is determined by requiring the electron distribution function to satisfy the boundary conditions described below.

At the two outer surfaces, α and β, the boundary conditions are

$$\begin{aligned} g^+_{1\sigma}&=P_{\alpha\sigma}g^-_{1\sigma} \quad \text{at } z=0\ ,\\ g^-_{3\sigma}&=P_{\beta\sigma}g^+_{3\sigma} \quad \text{at } z=d\ , \end{aligned} \tag{5}$$

where $d=d_1+d_2+d_3$ is the total thickness of the sandwich. The specularity factors, $P_{\alpha\sigma}$ and $P_{\beta\sigma}$ for the respective surfaces and for electrons of spin σ, take values between zero (completely diffusive scattering) and 1 (completely specular scattering) and provide a measure of the surface roughness. In Eq. (5), and in the boundary conditions at the interfaces in (6) below, the explicit functional dependence of the distribution functions $g^{\pm}_{i\sigma}$ has been dropped.

The boundary conditions for the potential (nondiffusive) scattering at the interfaces A and B take the form

$$\begin{aligned} g^-_{1\sigma}&=S_{A\sigma}R_{12\sigma}g^+_{1\sigma}+S_{A\sigma}T_{21\sigma}g^-_{2\sigma} \quad \text{at } z=d_1\ ,\\ g^+_{2\sigma}&=S_{A\sigma}R_{21\sigma}g^-_{2\sigma}+S_{A\sigma}T_{12\sigma}g^+_{1\sigma} \quad \text{at } z=d_1\ , \end{aligned} \tag{6}$$

$$\begin{aligned} g^-_{2\sigma}&=S_{B\sigma}R_{23\sigma}g^+_{2\sigma}+S_{B\sigma}T_{32\sigma}g^-_{3\sigma} \quad \text{at } z=d_1+d_2\ ,\\ g^+_{3\sigma}&=S_{B\sigma}R_{32\sigma}g^-_{3\sigma}+S_{B\sigma}T_{23\sigma}g^+_{2\sigma} \quad \text{at } z=d_1+d_2\ . \end{aligned}$$

Here $S_{A\sigma}$ and $S_{B\sigma}$, which vary between zero and 1, are factors that indicate the degree of potential scattering at each of the interfaces A and B for spin σ. The scattering follows the reflection-refraction laws when $S=1$ and is completely diffusive when $S=0$. The notation used for the transmission T and the reflection R coefficients is the following: $T_{ij\sigma}\equiv$ probability for an electron of spin σ in layer i to be transmitted (refracted) into layer j; $R_{kl\sigma}\equiv$ probability for an electron of spin σ in layer k with a velocity directed towards layer l to be reflected back into layer k. The equations and boundary conditions as written satisfy all the necessary conservation laws.

The functional dependence of the coefficients was determined by matching the free-electron-like (plane-wave) functions and their derivatives at each interface. The solution to this problem, which is identical to that encountered in optics for an interface between two media with different indices of refraction, is shown schematically in Fig. 2. The reflection R and transmission T coefficients take the form[20]

$$R_{ij\sigma}(E,\theta)=\left|\frac{1-h_{ij\sigma}(E,\theta)}{1+h_{ij\sigma}(E,\theta)}\right|^2\ ,$$

$$T_{ij\sigma}(E,\theta)=\frac{4\,\mathrm{Re}[h_{ij\sigma}(E,\theta)]}{|1+h_{ij\sigma}(E,\theta)|^2}=1-R_{ij\sigma}(E,\theta)\ .$$

Here θ is the angle of incidence, measured with respect to the z axis, of an electron of energy $E=\frac{1}{2}m_{i\sigma}v^2+V_{i\sigma}$ in layer i with spin σ and velocity v moving in a constant potential $V_{i\sigma}$. The scattering is completely elastic, i.e.,

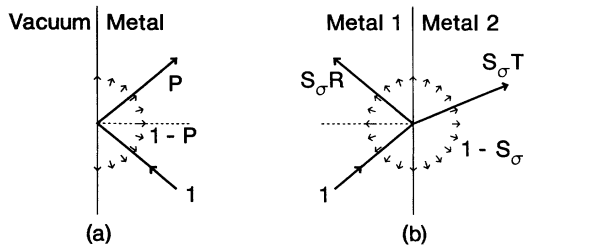

FIG. 2. Schematic diagrams of the scattering processes at (a) the vacuum-metal free surface and (b) the metal-metal interface. The parameters P and S_σ define the fractions controlled by the potentials. In (b) $S_\sigma R$ is the probability of specular scattering; $S_\sigma T$ is the probability of transmission (refraction) into the other metal. The isotropic, diffuse scattering parts are $(1-P)$ and $(1-S_\sigma)$, respectively.

the energy of the electron is a constant of the motion. The symbol Re means "the real part of"; the function $h_{ij\sigma}(E,\theta)$ has the form

$$h_{ij\sigma}(E,\theta)=\frac{\left[\frac{E-V_{j\sigma}}{E-V_{i\sigma}}-\sin^2\theta\right]^{1/2}}{\cos\theta} .$$

The transmission and reflection coefficients appearing in Eq. (6) are related by

$$R_{ij\sigma}(E,\theta_i)=R_{ji\sigma}(E,\theta_j) ,$$

$$T_{ij\sigma}(E,\theta_i)=T_{ji\sigma}(E,\theta_j) ,$$

where

$$\frac{\sin\theta_i}{\sin\theta_j}=\left[\frac{E-V_{j\sigma}}{E-V_{i\sigma}}\right]^{1/2} ;$$

this is a consequence of the principle of (optical) reversibility.

Substitution of Eq. (4) into the boundary equations (5) and (6) yields unique solutions of $F^{\pm}_{i\sigma}(\mathbf{v})$. The form of the boundary conditions is such that these functions depend only on the magnitude of the velocity v and the cosine of its angle with respect to the z axis. Therefore, the functions can be written as $F^{\pm}_{i\sigma}(v,\cos\theta)$ where the plus sign corresponds to $0\le\theta\le\pi/2$ and the minus sign corresponds to $\pi/2<\theta\le\pi$.

The current density along the electric field in each layer i for electrons with spin σ is given by

$$J_{xi\sigma}(z)=-|e|\left[\frac{m_{i\sigma}}{h}\right]^3\int v_x g_{i\sigma}(\mathbf{v},z)d^3\mathbf{v} , \tag{7}$$

where h is Planck's constant. Substitution of Eq. (4) into Eq. (7) and the use of Fermi-Dirac statistics yields

$$J_{xi\sigma}(z)=\sigma_{i\sigma}E\left\{1+\frac{3}{4}\int_{-1}^{1}\tilde{F}_{i\sigma}(u)(1-u^2)e^{-z/\lambda_{i\sigma}u}du\right\} , \tag{8}$$

where the Fermi velocity $v_{Fi\sigma}$ is given by

$$v_{Fi\sigma}=\left[\frac{2(E_F-V_{i\sigma})}{m_{i\sigma}}\right]^{1/2} ,$$

for an electron with the Fermi energy E_F. The mean free path $\lambda_{i\sigma}$ is defined by $\lambda_{i\sigma}\equiv v_{Fi\sigma}\tau_{i\sigma}$. The bulk conductivity of electrons from layer i of spin σ is denoted by $\sigma_{i\sigma}$ and is given by

$$\sigma_{i\sigma}=\frac{4}{3}\pi e^2\tau_{i\sigma}(m_{i\sigma})^2\left[\frac{v_{Fi\sigma}}{h}\right]^3 .$$

The function $\tilde{F}_{i\sigma}(u)$ is defined by the equation[21]

$$\tilde{F}_{i\sigma}(u)=\begin{cases}F^{+}_{i\sigma}(v_{Fi\sigma},u) & \text{if } u\ge 0 ,\\ F^{-}_{i\sigma}(v_{Fi\sigma},u) & \text{if } u<0 .\end{cases}$$

Physically the first term in Eq. (8) corresponds to the current in a solid of infinite extent with no surfaces or interfaces. The second term is a measure of the deviation in the current caused by the presence of surfaces and interfaces. Plots are shown below which show how the current is distributed throughout the trilayer. In order to obtain the MR, one requires the effective conductivity, which is found by averaging over the whole film

$$\sigma=\frac{1}{Ed}\sum_{i=1}^{i=3}\sum_{\sigma=\uparrow,\downarrow}\int J_{xi\sigma}(z)dz .$$

Integration yields

$$\sigma=\sum_{i=1}^{3}\sum_{\sigma=\uparrow,\downarrow}\sigma_{i\sigma}\left[\left[\frac{d_i}{d}\right]-\frac{3}{4}\left[\frac{\lambda_{i\sigma}}{d}\right]\int_{-1}^{1}du(1-u^2)u\tilde{F}_{i\sigma}(u)\{e^{-z_i/\lambda_{i\sigma}u}-e^{-z_{i-1}/\lambda_{i\sigma}u}\}\right] , \tag{9}$$

where $z_0=0$, $z_1=d_1$, $z_2=d_1+d_2$, and $z_3=d$. The first term in Eq. (9) can be interpreted as the bulk conductivity of each layer weighted by its relative thickness. The exponential factors in Eqs. (8) and (9), which go to infinity as $u\to 0^-$, are compensated by the prefactor $\tilde{F}_{i\sigma}(u)$, which approaches zero rapidly enough in the same limit to insure integrability.

The MR, $(\Delta\rho/\rho)$, is found by calculating independently the conductivities $\sigma_{\uparrow\downarrow}$ and $\sigma_{\uparrow\uparrow}$. Although in some cases the ferromagnetic layers may be different, in all results presented here it was assumed that the ferromagnetic layers 1 and 3 are composed of the same material with identical bulk properties. This assumption reduces the number of parameters necessary to characterize a structure. Associated with the electrons in layers 1 and 3 are the minority (denoted using a small subscript m) and the majority (denoted using a capital subscript M) spins with effective masses m_m and m_M, relaxation times τ_m and τ_M, and potentials V_m and V_M. The spin-up and spin-down electrons in layer 2, which is the normal-metal or spacer layer, move in a potential V_s with an effective mass m_s and relaxation time τ_s. At the outer surfaces α and β of the ferromagnetic layers 1 and 3, respectively, the surface scattering parameters for the majority and the minority spins are described by $P_{\alpha M}$, $P_{\beta M}$, $P_{\alpha m}$, and $P_{\beta m}$. At the 1-2 and 2-3 interfaces A and B, respectively, S_{AM}, S_{BM}, S_{Am}, and S_{Bm} describe the interfacial scattering of the majority and the minority spins.

The values of the potentials are determined by treating all of the valence s and d electrons as being in a single free-electron-like band with an isotropic effective mass. The effective mass is, in general, taken to be larger than the electron mass, since the d electrons, which contribute to the density of electrons, are in narrower bands than the free-electron-like s electrons. Within the ferromagnetic layers 1 and 3, the bands for the minority and the

majority spins are shifted by a k-independent exchange potential, yielding two different spin-dependent, constant potentials, V_m and V_M. The value of the exchange splitting is chosen so that the difference in the density of the majority and the minority electrons yields the net magnetic moment of the bulk ferromagnetic material.

III. RESULTS

The theory, as developed thus far for a sandwich of two identical ferromagnetic metals separated by a layer of a normal metal, includes 20 parameters: three effective masses m_M, m_m, and m_s; three constant potentials V_M, V_m, and V_s; three relaxation times τ_M, τ_m, and τ_s; three thicknesses d_1, d_2, and d_3; four free-surface scattering parameters $P_{\alpha M}$, $P_{\alpha m}$, $P_{\beta M}$, and $P_{\beta m}$; and four interface scattering parameters S_{AM}, S_{Am}, S_{BM}, and S_{Bm}.

The results presented here include only the cases for which the *relaxation times* are identical $\tau \equiv \tau_m = \tau_M = \tau_s$. (The *mean free paths* of the minority and the majority spins within the ferromagnetic layers 1 and 3 and for the spacer metal are still different, however, since the Fermi velocities are different.) The discussion of the results is also confined to the situation $d_F \equiv d_1 = d_3$ and $d_s \equiv d_2$, since this is the most common case. At the outer surfaces all P's are taken to be identical $P \equiv P_{\alpha M} = P_{\alpha m} = P_{\beta M} = P_{\beta m}$. The spin dependence of these parameters is caused mostly by magnetic impurities, which are taken not to be present at the outer (identical) surfaces. The interfaces are also assumed to be identical $S_M \equiv S_{AM} = S_{BM}$; $S_m \equiv S_{Am} = S_{Bm}$.

Results are given for two different multilayer systems, Fe-Cr and Fe-Cu. In these three metals the isotropic effective mass is assumed to be independent of the material and spin orientation with a value $m_M = m_m = m_s = 4.0 \times$ free-electron mass. With this effective mass the potentials, with respect to the Fermi energy E_F chosen to be at $E_F = 0$, are

$$V_M = -8.23 \text{ eV}, \quad V_m = -5.73 \text{ eV} \quad \text{for Fe},$$

$$V_s = -5.77 \text{ eV} \quad \text{for Cr},$$

$$V_s = -8.54 \text{ eV} \quad \text{for Cu}.$$

Figure 3 shows the potential energies: V_M, V_m, and V_s for Fe-Cu for the spin-up and spin-down electrons for both the parallel and the antiparallel configurations.

The parameters that remain to be specified for each case (Fe-Cr and Fe-Cu) are altogether six: (a) two geometric parameters d_F and d_s; (b) one relaxation time τ, which depends on bulk sample properties; (c) one outer-surface scattering parameter P (the roughness of the outer surfaces); and (d) two interface scattering parameters S_M, S_m (diffuse scattering versus potential scattering at the interfaces for the majority and the minority spins, respectively).

Even with these specifications, the phenomena under consideration are complicated functions of the six variables, and the task of describing these dependencies is not simple. In general terms, and with exceptions, it is found that $(\Delta\rho/\rho)$ is a strong function of the surface and interface parameters P, S_M, and S_m, and a relatively weak function of the thicknesses and the mean free path. For example, as P, S_M, and S_m vary between 0 and 1, the calculated $(\Delta\rho/\rho)$ varies between 0 and 92.7 % for Fe-Cr trilayers and 0 and 94.4 % for Fe-Cu trilayers, when values of $d_F = d_s = 10.0$ Å and $\tau = 5.0 \times 10^{-13}$ s are chosen. Figures 4 and 5 show the regions in this three-dimensional "surface and interfacial" parameter space where $(\Delta\rho/\rho)$ is greater than 20 % for these values of d_F, d_s, and τ. With this choice of τ, the mean free paths are: (i) 4 250 Å for the majority-spin and 3 540 Å for the minority-spin electrons in Fe; (ii) 3 560 Å for electrons in Cr; and (iii) 4 330 Å for electrons in Cu. These values correspond to all mean free paths that are orders of magnitude larger than the film thicknesses, i.e., the clean-film limit, where surface and interface effects are supposed to be paramount.

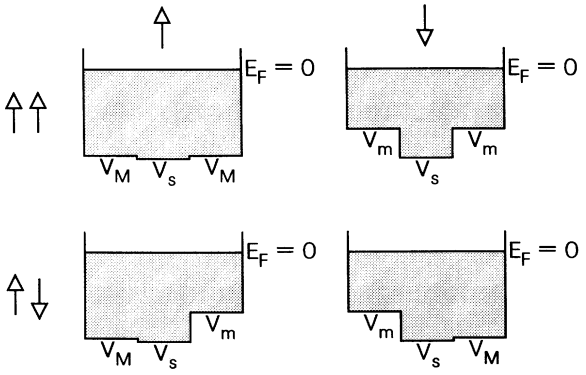

FIG. 3. Schematic diagrams of the potentials for the spin ↑ and spin ↓ electrons in the parallel (↑↑) and the antiparallel (↑↓) configurations of an Fe-Cu-Fe trilayer.

Some of the interesting results of the calculations are illustrated in Figs. 4–11. It was found in general that:

(a) $(\Delta\rho/\rho)$ increases with increasing values of P, except

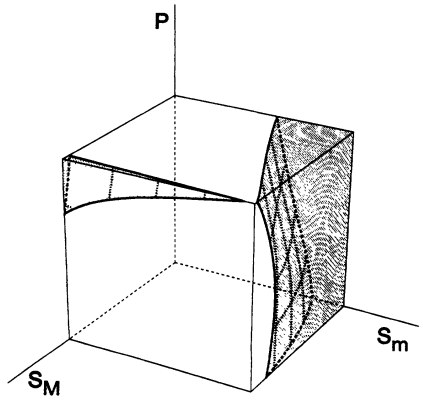

FIG. 4. The region in three-dimensional parameter space (P, S_M, S_m) where $(\Delta\rho/\rho) > 0.2$ for the parameters corresponding to Fe-Cr and $d_F = d_s = 10$ Å, and $\tau = 5.0 \times 10^{-13}$ s. The three parameters vary between 0 and 1.

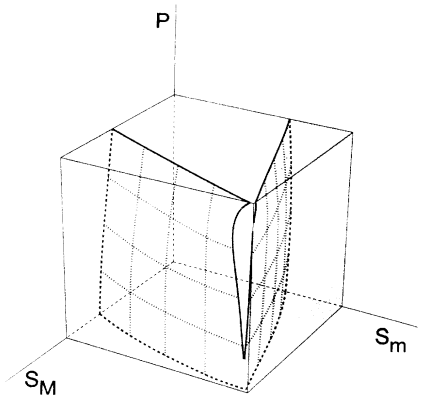

FIG. 5. Region in three-dimensional parameter space (P,S_M,S_m) where $(\Delta\rho/\rho)>0.2$ for the parameters corresponding to Fe-Cu and $d_F=d_s=10$ Å, and $\tau=5.0\times10^{-13}$ s. The three parameters vary between 0 and 1.

in the region where $S_M\approx S_m\approx 1$ (see Fig. 6).

(b) $(\Delta\rho/\rho)$ is in general small (only a few percent) when $S_M=S_m$, except when both parameters are very close to 1 (see Figs. 4, 5, and 7).

(c) $(\Delta\rho/\rho)$, as a function of d_F, exhibits a variety of behaviors which include (i) a monotonic decrease with increasing d_F; (ii) an initial increase followed by a decrease (a single maximum); (iii) a decrease, followed by an increase and a subsequent decrease (a minimum followed by a maximum); in all cases the asymptotic value as $d_F\rightarrow\infty$ is zero (see Fig. 8).

(d) $(\Delta\rho/\rho)$, as a function of increasing d_s, exhibits either (i) a continuous monotonic decrease, or, most commonly, (ii) a single maximum[22] at a value of d_s of the order of d_F; the asymptotic value as $d_s\rightarrow\infty$ is also zero (see Fig. 9).

(e) $(\Delta\rho/\rho)$, as a function of the relaxation time τ, either (i) increases monotonically and saturates at a maximum value, or, most commonly, (ii) increases to a maximum, and then *very gradually* decreases (see Fig. 10).

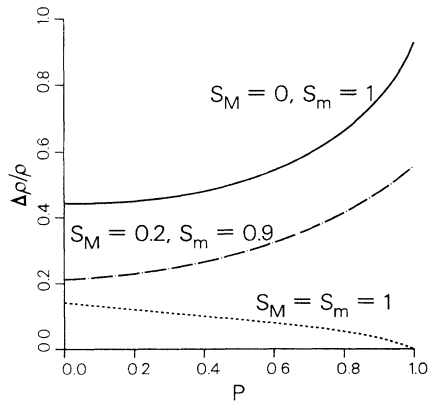

FIG. 6. Variation of $(\Delta\rho/\rho)$ as a function of P for the parameters of Fe-Cr, $\tau=5.0\times10^{-13}$ s, $d_F=d_s=10$ Å, and various values of S_M, and S_m.

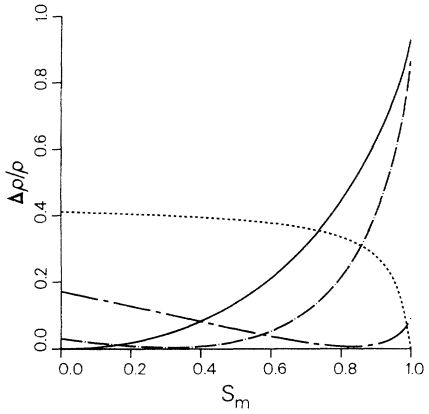

FIG. 7. Variation of $(\Delta\rho/\rho)$ as a function of S_m for the parameters of Fe-Cr, $\tau=5.0\times10^{-13}$ s, $d_F=d_s=10$ Å, and four different values of S_M and P: (1) chain-dashed curve $S_M=1$ and $P=0.5$; (2) dashed curve $S_M=1$ and $P=1$; (3) chain-dotted curve $S_M=0.5$ and $P=1$; and (4) solid curve $S_M=0$ and $P=1$.

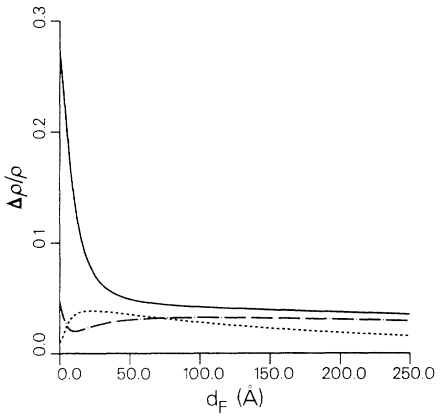

FIG. 8. Variation of $(\Delta\rho/\rho)$ as a function of d_F for the parameters of Fe-Cr, $d_s=10$ Å, $\tau=5.0\times10^{-13}$ s and three different values of S_M, S_m, and P: (1) chain-dotted curve $S_M=S_m=0.8$ and $P=0$; (2) dashed curve $S_M=S_m=0.8$ and $P=1$; and (3) solid curve $S_M=S_m=1$ and $P=0$.

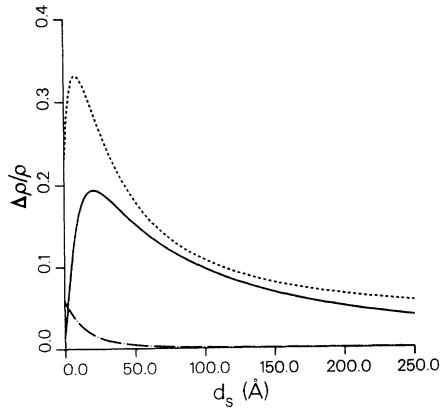

FIG. 9. Variation of $(\Delta\rho/\rho)$ as a function of d_s for the parameters of Fe-Cr, $d_F=10$ Å, $\tau=5.0\times10^{-13}$ s and three different values of S_M, S_m, and P: (1) chain-dotted curve $S_M=S_m=0.9$ and $P=1$; (2) dashed curve $S_M=0.5$, $S_m=1$, and $P=0.5$; and (3) solid curve $S_M=1$, $S_m=0$, and $P=0$.

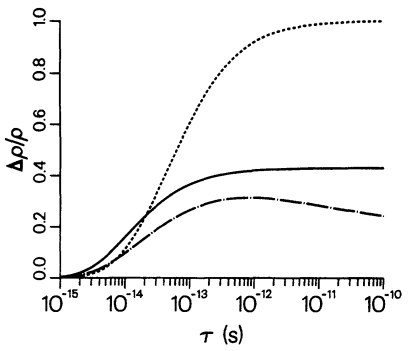

FIG. 10. Variation of $(\Delta\rho/\rho)$ as a function of τ for the parameters of Fe-Cr, $d_s = d_F = 10$ Å, $P = 1$, and three different values of S_M and S_m: (1) chain-dotted curve $S_M = 0$ and $S_m = 0.7$; (2) dashed curve $S_M = 0.5$ and $S_m = 1$; and (3) solid curve $S_M = 1$ and $S_m = 0$.

Figures 4 and 5 contain information on how, for specific values of d_F, d_s, and τ, the quality of surfaces and interfaces influences the MR. As the surface scattering parameter P increases from 0 to 1, i.e., as the scattering becomes less diffuse (or, equivalently, the surface roughness decreases) the MR in general increases. It is also evident from these two figures that the region of large MR is close either to the plane $S_M = 1$, or to the plane $S_m = 1$, and away from the plane $S_M = S_m$. There is a very large asymmetry between S_M and S_m in Fe-Cr, but considerably less so in Fe-Cu.

It is interesting to note that when $P = 1$, the MR of the trilayer becomes identical to that of an infinite multilayer or superlattice. A specular-scattering event makes the electron traverse the same ferromagnetic layer for a second time in the opposite direction or, equivalently, "continue" through a mirror image of the film. Therefore, if for both surfaces $P = 1$, then as far as the MR is concerned, a trilayer

$$\text{vacuum}|d_F|d_s|d_F|\text{vacuum}$$

is exactly equivalent to an infinite, periodic superstructure

$$\cdots |2d_F|d_s|2d_F|d_s|2d_F|d_s|2d_F|\cdots .$$

As seen above, the MR increases in general with P, because the number of interfaces where magnetic scattering can occur "increases" as P increases. When realistic values are chosen for the parameters, the MR is found to increase by as much as an order of magnitude when P increases from 0 to 1. This fact can be reinterpreted as an increase in the MR as the number of magnetic interfaces encountered by an electron within its bulk mean free path increases.

Experimentally it is found that the more layers a sample has, the larger the MR. The (liquid-He temperature) MR in Fe-Cr trilayers prepared by molecular-beam-epitaxy methods is found to be a few percent,[23] while the MR is found to be nearly 50% Fe-Cr in *multilayers* prepared by the same method at the same temperature.[4]

IV. DISCUSSION AND CONCLUSIONS

Figure 4 shows a marked asymmetry in the dependence of $(\Delta\rho/\rho)$ on S_M and S_m, i.e., the majority- and minority-spin interface scattering have a very different effect on the MR. By contrast, a large asymmetry is not present for Fe-Cu (Fig. 5). Figure 3 shows the potential energies for Fe-Cu for both the parallel and the antiparallel configurations. It is seen that

$$|V_s| \approx |V_M| < |V_m| .$$

On the other hand, the bottom of the band for Cr is lower than but much closer to that for the minority spins in iron, i.e., in the Fe-Cr samples

$$|V_M| < |V_s| \approx |V_m| .$$

The difference in V_s has a large effect on the MR, as can be seen in the plots of the in-plane current distribution across the trilayers. Shown in Fig. 11 are the in-plane currents for the parallel (Pl) and the antiparallel (An) configurations of Fe-Cr with $S_M = 0$, $S_m = 1$, and $P = 0.5$; the contributions to the current of spin-up and spin-down electrons are plotted separately. For the chosen set of parameters the $(\downarrow_{\text{Pl}})$ electrons undergo completely nondiffusive scattering at both interfaces, whereas $(\downarrow_{\text{An}})$ electrons and the $(\uparrow)$ electrons in both configurations undergo completely diffusive scattering either at one or at both interfaces. The current carried by the $(\downarrow_{\text{Pl}})$ electrons is the largest of the four contributions because those electrons are, in fact, never "randomized" at the interfaces, i.e., their current is not degraded by diffusive interface scattering. The fact that $(\Delta\rho/\rho)$ is determined by the difference of the conductivities of the parallel and the an-

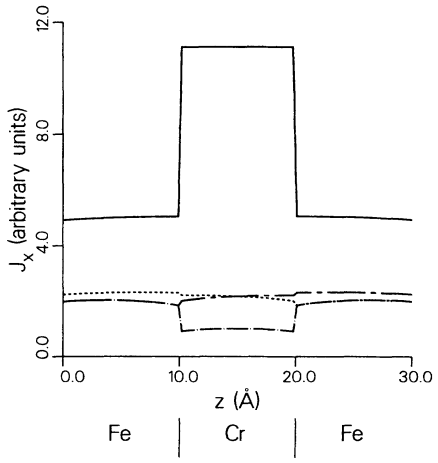

FIG. 11. Distribution of the in-plane current (J_x) (plotted in arbitrary units) over the thickness of an Fe-Cr-Fe trilayer. The contribution to the current from the spin-up and the spin-down electrons is plotted in the parallel and the antiparallel configuration of the Fe-layer magnetic moments: (1) solid curve is the $(\downarrow_{\text{Pl}})$ electrons; (2) chain-dotted curve is the $(\uparrow_{\text{Pl}})$ electrons; (3) dashed curve is the $(\downarrow_{\text{An}})$ electrons; (4) chain-dashed curve is the $(\uparrow_{\text{An}})$ electrons. The values of the parameters are $\tau = 5.0 \times 10^{-13}$, $d_F = d_s = 10$ Å, $S_M = 0$, $S_m = 1$, and $P = 0.5$.

tiparallel configurations, which are each proportional to the sum of the currents carried by the spin-up and spin-down electrons, explains why $(\Delta\rho/\rho)$ is large (50.6%) in this case.

A fraction of the $(\downarrow_{\mathrm{Pl}})$ electrons in the Cr layer, those incident at low grazing angles upon the Fe-Cr interfaces, are totally internally reflected, since $|V_s| < |V_m|$. These electrons scatter diffusively only within the *bulk* of the Cr layer and so are able to follow long trajectories (a full mean free path) before being scattered.[24] This phenomenon leads to a "channeling effect" within the Cr layer. It explains why the current carried by the $(\downarrow_{\mathrm{Pl}})$ electrons is larger in the Cr layer than in the Fe layers.

Figure 12 shows how the in-plane current is distributed across another Fe-Cr trilayer, but for $S_M=1$, $S_m=0$, and $P=0.5$ of Fig. 4. In this case only the $(\uparrow_{\mathrm{Pl}})$ electrons are scattered nondiffusely at both interfaces. Since $|V_s| < |V_M|$, channeling does not occur in the Cr layer, and the current is actually larger within the Fe layers. Channeling can only take place in the Fe layers and only when P is close to 1. Therefore the regions where the MR is large, i.e., $(\Delta\rho/\rho) > 0.2$, when S_M is close to 1, are clustered around $P=1$. Even when P is close to 1, the MR is not very large; channeling occurs in *only one* of the Fe layers for both the $(\uparrow_{\mathrm{An}})$ and $(\downarrow_{\mathrm{An}})$ electrons. Thus the difference $(\sigma_{\uparrow\uparrow}-\sigma_{\uparrow\downarrow})$ in Eq. (1) for $S_M=1$, $S_m=0$, and $P=1$ is considerably smaller, $(\Delta\rho/\rho)=0.411$, than that for $S_M=0$, $S_m=1$, and $P=1$, $(\Delta\rho/\rho)=0.927$.

In the Fe-Cu trilayer, since $|V_s|$ is greater than $|V_M|$ and $|V_m|$, channeling occurs in the Cu layer when either S_M or S_m are close to 1 for the $(\uparrow_{\mathrm{Pl}})$ or the $(\downarrow_{\mathrm{Pl}})$ electrons, respectively. Channeling within the Cu layer, for either S_M or S_m close to 1, leads to a large MR and to the symmetric-looking plot of Fig. 5.

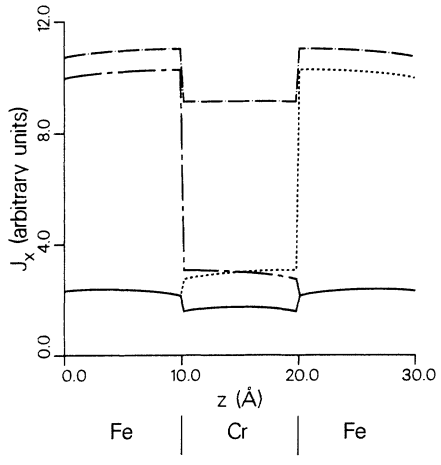

FIG. 12. Distribution of the in-plane current (J_x) (plotted in arbitrary units) over the thickness of an Fe-Cr-Fe trilayer. The contribution to the current from the spin-up and the spin-down electrons is plotted in the parallel and the antiparallel configuration of the Fe-layer magnetic moments: (1) solid curve is the $(\downarrow_{\mathrm{Pl}})$ electrons; (2) chain-dotted curve is the $(\uparrow_{\mathrm{Pl}})$ electrons; (3) dashed curve is the $(\downarrow_{\mathrm{An}})$ electrons; (4) chain-dashed curve is the $(\uparrow_{\mathrm{An}})$ electrons. The values of the parameters are: $\tau=5.0\times10^{-13}$, $d_F=d_s=10$ Å, $S_M=1$, $S_m=0$, and $P=0.5$.

Interesting surface and size effects occur when both S_M and S_m are close to 1. The vacuum-metal interfaces now dominate the scattering processes, and the MR actually decreases as P increases, as can be seen in Figs. 5 and 6. For well-formed interfaces, i.e., for $S_\sigma \approx 1$, the MR is enhanced by greater surface roughness. For smoother surfaces, as P approaches 1, the current within the Fe layers increases relative to that within the Cu layers. In the extreme case when all three $P=S_M=S_m=1$, the current within each layer for each spin is directly proportional to the density of electrons of that spin in that layer, i.e., to $|V_{i\sigma}|^{3/2}$. Under these conditions the size effect disappears, and the MR vanishes. The trilayer becomes a superlattice with no diffusive scattering at the interfaces. This result, $(\Delta\rho/\rho)=0$ for $P=S_M=S_m=1$, is valid for any combination of materials and for all values of d_i and τ (or any other of the geometric and intrinsic metal parameters of the general model).[25] It follows from the fact that potential scattering of the electrons at the interface is completely microscopically reversible, so that the conductivity of the multilayer is equal to the sum of the bulk conductivities in each layer independently.

In the opposite case, when $S_\sigma=0$ for all interfaces (i.e., rough interfaces with completely diffusive scattering), $(\Delta\rho/\rho)=0$ once again, this time regardless of the value of P, the types of materials in the trilayer, or the values of any other parameters. In this case there is no coherence between the ferromagnetic layers. The individual layers are uncoupled and the conductance of the trilayer becomes equal to the sum of the conductances of three layers having rough surfaces, $P=0$ (this is the case obtained analytically in Ref. 15).

The experimentally observed values of MR in Fe-Cr and Fe-Cu multilayers can be matched by the calculation with a proper choice of the parameters. However, the model in its present form, which considers all of the valence s and d electrons as comprising a single band with a single isotropic effective mass, yields effective resistivities $\rho_{\uparrow\uparrow}$ and $\rho_{\uparrow\downarrow}$, which are about an order of magnitude smaller than those measured in multilayer structures. The effective resistivities are too small because the model has too many free-electron-like conduction electrons: eight in Fe, six in Cr, and 11 in Cu. Proper consideration must be taken of the fact that, in these metals, s and d electrons contribute very differently to the transport properties. The narrow character of the d bands has been accounted for in the single-band approach by a single, large, isotropic effective mass, four times larger than the free-electron mass. A better approach to the problem would be to include a realistic band structure with its 12 bands, wide and narrow, as well as the hybridization and spin polarization. Such a treatment would make the calculations much more involved, if not impossible.

Within the confines of a single-band model a simple, natural way to decrease the number of conduction electrons is by reducing the density of the electrons in each layer by a constant scaling factor γ independent of the material and the spin of the electron. It should be stressed that the introduction of such a scaling factor

does not change the form of the results found above. The number of electrons and the magnetization decrease by a factor of γ. The resistivities $\rho_{\uparrow\uparrow}$ and $\rho_{\uparrow\downarrow}$ increase by a factor of about γ, and $(\Delta\rho/\rho)$ decreases by a factor of about $\gamma^{1/3}$. A value of $\gamma=8$ was chosen for making comparisons with experimental data. With this value the number of effective free-electron-like conduction electrons is 1.00 in Fe, 0.75 in Cr, and 1.38 in Cu. Calculations were able to yield values of the MR and the resistivities, $\rho_{\uparrow\uparrow}$ and $\rho_{\uparrow\downarrow}$, similar to those measured experimentally.

In order to model multilayers, which consist of several layers, the surface parameter P is taken to be 1. Baibich *et al.*[4] found that a multilayer of (Fe 30 Å/Cr 9 Å)$_{60}$, prepared by molecular-beam epitaxy, had $(\Delta\rho/\rho)\approx 0.46$ and an absolute resistivity change of about 23 $\mu\Omega$ cm. With $P=1$, $S_m=0$, $S_M=1$, $d_F=30$ Å, $d_s=9$ Å, and $\tau=1\times10^{-13}$ s values of $\rho_{\uparrow\uparrow}=26.1$ $\mu\Omega$ cm and $\rho_{\uparrow\downarrow}=47.6$ $\mu\Omega$ cm were calculated, which corresponds to $(\Delta\rho/\rho)=0.452$ for the MR. When P is set equal to zero, with the values for the other parameters unchanged, calculations yield $\rho_{\uparrow\uparrow}=63.5$ $\mu\Omega$ cm, $\rho_{\uparrow\downarrow}=74.2$ $\mu\Omega$ cm, and $(\Delta\rho/\rho)=0.144$ for the MR. Experimental values of ρ are between 20 and 80 $\mu\Omega$ cm. With this choice of γ, τ, and effective mass (i.e., an effective mass of four times the electron mass), the bulk mean free paths are: 425 Å for the majority-spin and 354 Å for the minority-spin electrons in Fe; and 356 Å for the electrons in Cr.

Pétroff *et al.*[18] report that a multilayer (Fe 15 Å/Cu 15 Å)$_{60}$ made by sputtering had the following characteristics: $\rho_{\uparrow\uparrow}=24.8$ $\mu\Omega$ cm, $\rho_{\uparrow\downarrow}=27.8$ $\mu\Omega$ cm, and $(\Delta\rho/\rho)=0.108$. With $P=1$, $S_m=0.72$, $S_M=0.93$, $d_F=d_s=15$ Å, and $\tau=1\times10^{-13}$ s, values of $\rho_{\uparrow\uparrow}=24.1$ $\mu\Omega$ cm and $\rho_{\uparrow\downarrow}=27.0$ $\mu\Omega$ cm were calculated, which correspond to $(\Delta\rho/\rho)=0.107$. Here the bulk mean free paths are: 425 Å for the majority-spin and 354 Å for the minority-spin electrons in Fe; and 433 Å for the electrons in Cr.

Calculations predict that a trilayer with completely diffuse scattering at the surface, $P=0$, and with atomically clean interfaces, $S_M=S_m=1$, can have a sizable MR (caused by the "channeling effect" discussed above) when the density of spin-up and/or the spin-down electrons is greater in the spacer layer than the corresponding ones in the outer *ferromagnetic* layers. For example in Fe-Cu, where the density of electrons is greatest in the Cu layer, the results $\rho_{\uparrow\uparrow}=10.1$ $\mu\Omega$ cm, $\rho_{\uparrow\downarrow}=16.3$ $\mu\Omega$ cm, and $(\Delta\rho/\rho)=0.382$ were found when $\gamma=8$, $d_F=d_s=10$ Å and $\tau=5\times10^{-13}$ s.

As clearly seen in Figs. 4 and 5, a large MR requires, in general, a large difference in interface scattering for the different spins. When $S_M=S_m$ (with some exceptions, see Fig. 5 and the size effect discussed above), the MR is found to be not more than a few percent. Therefore a large MR cannot be explained as being caused solely by different densities of electrons with different spins, which vary from layer to layer. What is required is a spin imbalance *and* a spin-dependent scattering mechanism at the interface, i.e., $S_M\neq S_m$. When such a spin-dependent scattering mechanism exists, for example when magnetic impurities are present at the interfaces, the MR is profoundly influenced by spatial variations in the density of electron spins. This is the main cause of the GMR effect in ferromagnetic multilayers.

ACKNOWLEDGMENTS

We acknowledge helpful discussions with A. da Silva and P. Levy. R.Q.H. acknowledges the support of the Department of Education. This research was supported, at the Lawrence Berkeley Laboratory, by the Director, Office of Energy Research, Office of Basic Energy Sciences, Materials Sciences Division, U.S. Department of Energy, under Contract No. DE-AC03-76SF00098.

[1] *Thin Film Growth Techniques for Low-Dimensional Structures,* edited by R. F. C. Farrow, S. S. P. Parkin, P. J. Dobson, J. H. Neave, and A. S. Arrott (Plenum, New York, 1987).

[2] *Synthetic Modulated Structures,* edited by L. L. Chang and B. C. Giessen (Academic, New York, 1985); *Metallic Superlattices: Artificially Structured Materials,* edited by T. Shinjo and T. Takada, Studies in Physical and Theoretical Chemistry Vol. 49 (Elsevier, Amsterdam, 1987); B. Y. Jin and J. B. Ketterson, Adv. Phys. **38**, 189 (1989).

[3] S. S. P. Parkin, Phys. Rev. Lett. **67**, 3598 (1991).

[4] M. N. Baibich, J. M. Broto, A. Fert, F. Nguyen Van Dau, F. Pétroff, P. Etienne, G. Creuzet, A. Friederich, and J. Chazelas, Phys. Rev. Lett. **61**, 2472 (1988).

[5] S. S. P. Parkin, N. More, and K. P. Roche, Phys. Rev. Lett. **64**, 2304 (1990).

[6] J. Unguris, R. J. Celotta, and D. T. Pierce, Phys. Rev. Lett. **67**, 140 (1991).

[7] E. E. Fullerton, D. M. Kelly, J. Guimpel, I. K. Schuller, and Y. Bruynseraede, Phys. Rev. Lett. **68**, 859 (1992).

[8] P. Baumgart, B. A. Gurney, D. R. Wilhoit, T. Nguyen, B. Dieny, and V. Speriosu, J. Appl. Phys. **69**, 4792 (1991).

[9] A. Fert and I. A. Campbell, J. Phys. F **6**, 849 (1976); I. A. Campbell and A. Fert, in *Ferromagnetic Materials,* edited by E. P. Wohlfarth (North-Holland, Amsterdam, 1982), Vol. 3, p. 769.

[10] P. M. Levy, S. Zhang, and A. Fert, Phys. Rev. Lett. **65**, 1643 (1990).

[11] A. Barthélémy, A. Fert, M. N. Baibich, S. Hadjoudj, F. Pétroff, P. Etienne, R. Cabanel, S. Lequien, F. Nguyen Van Dau, and G. Creuzet, J. Appl. Phys. **67**, 5908 (1990).

[12] J. Barnaś, A. Fuss, R. E. Camley, P. Grünberg, and W. Zinn, Phys. Rev. B **42**, 8110 (1990).

[13] R. E. Camley and J. Barnaś, Phys. Rev. Lett. **63**, 664 (1989).

[14] K. Fuchs, Proc. Cambridge Philos. Soc. **34**, 100 (1938).

[15] E. H. Sondheimer, Adv. Phys. **1**, 1 (1952).

[16] E. C. Stoner, Proc. R. Soc. London Ser. A **165**, 372 (1938).

[17] G. G. Cabrera, and L. M. Falicov, Phys. Status Solidi B **61**, 539 (1974); **62**, 217 (1974).

[18] F. Pétroff, A. Barthélémy, D. H. Mosca, D. K. Lottis, A. Fert, P. A. Schroeder, W. P. Pratt, Jr., and R. Loloee, Phys. Rev. B **44**, 5355 (1991).

[19] It should be noted that the magnetoresistance $(\Delta\rho/\rho)$, as defined, is positive when it refers to what is usually called a negative MR. Only cases with $(\Delta\rho/\rho)\geq 0$ are considered in

this contribution. Situations where $(\Delta\rho/\rho)<0$ (ordinary magnetoresistance) may occur in the model when the relaxation times $\tau_{i\sigma}$ for spin σ take different values in different layers i. Such cases are not discussed here.

[20]For the sake of simplicity the formulas for the reflection and transmission coefficients are written exclusively for the case in which the effective masses are the same on both sides of the interface, i.e., $m_{i\sigma}=m_{j\sigma}$.

[21]It should be noted that the function $\tilde{F}_{i\sigma}(u)$ has an analytic form and can be written as a closed expression. The expression takes a somewhat simpler form for long mean free paths. It, however, contains in all instances the transmission and reflection coefficients and, when inserted in Eq. (9), it yields expressions too complicated to be evaluated analytically. For the sake of brevity the expression is not included here.

[22]The observed maxima in the magnetoresistance shown in Fig. 9 are caused by the fact that most of the effect is caused, as discussed below, by a channeling effect—within the spacer layer—of the spin for which $S=1$. As $d_s\rightarrow 0$ the contribution of the "channel" to the current becomes smaller, the electrons of both spins are subject in all configurations to the strong diffuse scattering of the free surfaces, and the magnetoresistance decreases with decreasing d_s.

[23]A. Chaiken, T. M. Tritt, D. J. Gillespie, J. J. Krebs, P. Lubitz, M. Z. Harford, and G. A. Prinz, J. Appl. Phys. **69**, 4798 (1991).

[24]It should be noted that the channeling effect, *per se,* does not necessarily lead to a large magnetoresistance, as can be seen from the case shown in Fig. 6 [$(\Delta\rho/\rho)=0$ for $P=S_M=S_m=1$]. The large magnetoresistance appears when, in the parallel arrangement, there is channeling for *only one spin* and diffuse interface scattering for the other one. In that case, in the antiparallel arrangement, both spins partake in the diffuse scattering, and the long electron trajectories (and the channeling) are lost.

[25]The particular result $(\Delta\rho/\rho)=0$ is valid for $P=S_M=S_m=1$ and for any combination of geometric and intrinsic metal parameters as long as $\tau_{i\sigma}=\tau_\sigma$, i.e., the relaxation times for each spin are *the same* in all layers of the system.

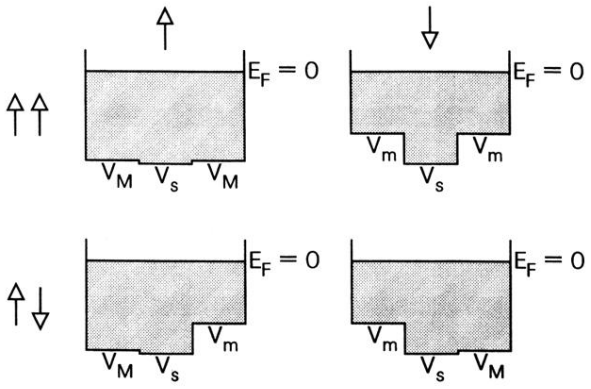

FIG. 3. Schematic diagrams of the potentials for the spin ↑ and spin ↓ electrons in the parallel (↑↑) and the antiparallel (↑↓) configurations of an Fe-Cu-Fe trilayer.

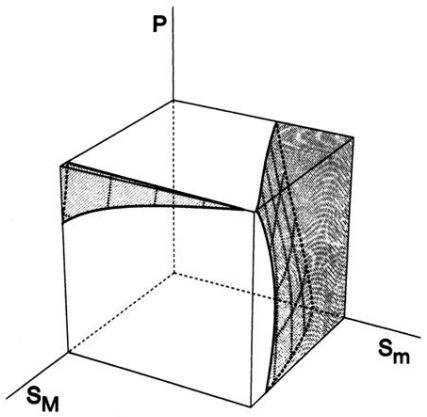

FIG. 4. The region in three-dimensional parameter space (P,S_M,S_m) where $(\Delta\rho/\rho)>0.2$ for the parameters corresponding to Fe-Cr and $d_F=d_s=10$ Å, and $\tau=5.0\times10^{-13}$ s. The three parameters vary between 0 and 1.

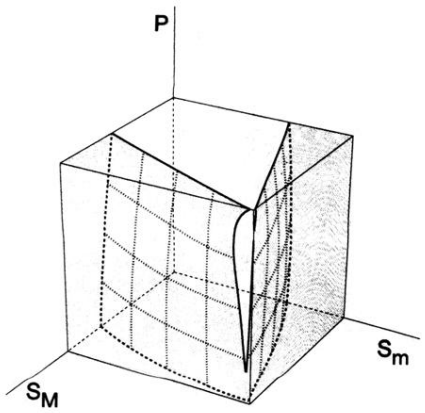

FIG. 5. Region in three-dimensional parameter space (P,S_M,S_m) where $(\Delta\rho/\rho)>0.2$ for the parameters corresponding to Fe-Cu and $d_F=d_s=10$ Å, and $\tau=5.0\times10^{-13}$ s. The three parameters vary between 0 and 1.